Magnetographic array for the capture and enumeration of single cells and cell pairs

C. Wyatt Shields IV,[1,2] Carissa E. Livingston,[1] Benjamin B. Yellen,[2,3] Gabriel P. López,[1,2,3,a)] and David M. Murdoch[4,a)]
[1]*Department of Biomedical Engineering, Duke University, Durham, North Carolina 27708, USA*
[2]*NSF Research Triangle Materials Research Science and Engineering Center, Durham, North Carolina 27708, USA*
[3]*Department of Mechanical Engineering and Materials Science, Duke University, Durham, North Carolina 27708, USA*
[4]*Department of Medicine, Duke University, Durham, North Carolina 27710, USA*

(Received 21 May 2014; accepted 16 June 2014; published online 1 July 2014)

We present a simple microchip device consisting of an overlaid pattern of micromagnets and microwells capable of capturing magnetically labeled cells into well-defined compartments (with accuracies >95%). Its flexible design permits the programmable deposition of single cells for their direct enumeration and pairs of cells for the detailed analysis of cell-cell interactions. This cell arraying device requires no external power and can be operated solely with permanent magnets. Large scale image analysis of cells captured in this array can yield valuable information (e.g., regarding various immune parameters such as the CD4:CD8 ratio) in a miniaturized and portable platform. © *2014 Author(s). All article content, except where otherwise noted, is licensed under a Creative Commons Attribution 3.0 Unported License*. [http://dx.doi.org/10.1063/1.4885840]

The emergent need for point-of-care devices has spurred development of simplified platforms to organize cells across well-defined templates.[1] These devices employ passive microwells, immunospecific adhesive islands, and electric, optical, and acoustic traps to manipulate cells.[2–6] In contrast, magnetic templating can control the spatial organization of cells through its ability to readily program ferromagnetic memory states.[7] While it has been applied to control the deposition of magnetic beads,[8–13] it has not been used to direct the deposition of heterogeneous cell pairs, which may help provide critical insight into the function of single cells.[14,15] As such, we developed a simple magnetographic device capable of arraying single cells and pairs of cells with high fidelity. We show this magnetic templating tool can use immunospecific magnetic labels for both the isolation of cells from blood and their organization into spatially defined wells.

We used standard photolithographic techniques to fabricate the microchips (see supplementary material[16]). Briefly, an array of 10×30 μm cobalt micromagnets were patterned by a photolithographic liftoff process and overlaid with a pattern of dumbbell-shaped microwells formed in SU-8 photoresist (Fig. 1(a)). The micromagnets were designed to produce a predominantly vertical field in the microwells by aligning the ends of the micromagnet at the center of each well of the dumbbell. These features were deposited across an area of ≈400 mm^2 (>50 000 well pairs per microchip) (Fig. 1(b)). Depending on the programmed magnetization state with respect to the external field, magnetic beads or cells were attracted to one pole and repelled by the other pole of each micromagnet, leading to a biased deposition (Fig. 1(c)).[12]

To demonstrate the capability of the array to capture cells into a format amenable for rapid image processing, we organized CD3+ lymphocytes using only hand-held permanent magnets. We isolated CD3+ lymphocytes from blood via positive selection using anti-CD3 magnetic

[a)]Authors to whom correspondence should be addressed. Electronic addresses: gabriel.lopez@duke.edu, Tel.: (+1) 919 660-5435, and david.murdoch@duke.edu, Tel.: (+1) 919 684-1106.

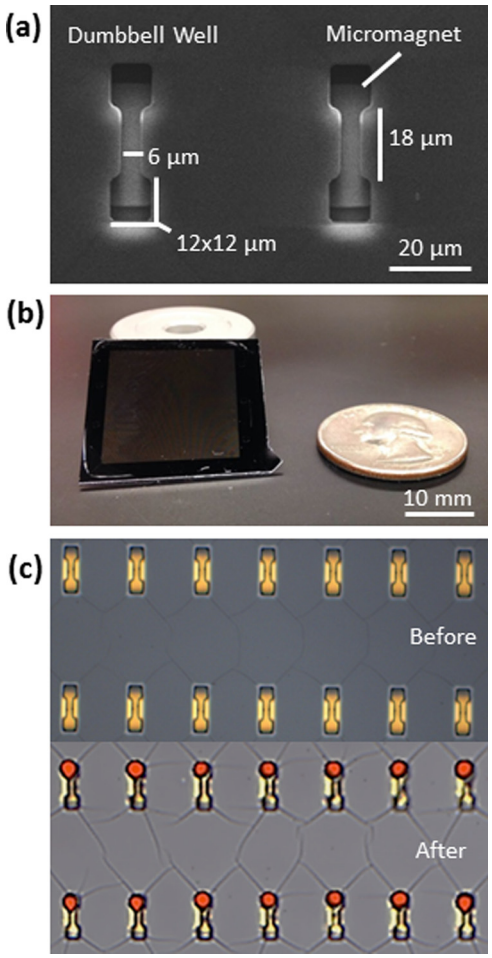

FIG. 1. Magnetographic array for single cell analysis. (a) SEM image of the dumbbell-shaped well pairs for capturing magnetically labelled cells. (b) Photograph of the finished device. (c) An array of well pairs displaying a pitch of 60×120 μm before (top) and 10 min after the deposition of magnetic beads (bottom).

nanoparticles (EasySep^{TM}, STEMCELL Technologies) with purities confirmed by flow cytometry (97.8%; see supplementary material[16]). We then stained 1×10^6 CD3+ cells with anti-CD8 Alexa-488 and anti-CD4 Alexa-647 (5 μl of each antibody in 100 μl for 20 min; BD Bioscience) to determine the CD4:CD8 ratio, a prognostic ratio for assessing the immune system.[17,18]

Variably spaced neodymium magnets (0.5 in. $\times$ 0.5 in. $\times$ 1 in.; K&J Magnetics, Inc.) were fixed on either side of the microchip to generate a tunable magnetic field (0–400 G; Fig. 2(a)). Using this setup, fluorescently labeled cells were deposited, and the populations of CD4+ and CD8+ cells were indiscriminately arrayed, imaged, and enumerated using ImageJ. The resulting CD4:CD8 ratio of 1.84 ± 0.18 (Fig. 2(b)) was confirmed by flow cytometry with a high correlation (5.4% difference; Fig. 2(c)), indicating the magnetographic microarray can pattern cells for the rapid and accurate assessment of critical phenotypical parameters without complex equipment (e.g., function generators or flow cytometers).

More complex operations, such as the programmed deposition of cell pairs, can be achieved by leveraging the switchable, bistable magnetization of the micromagnets for the detailed studies of cell-cell interactions (Figs. 3(a)–3(d)).[12] For these studies, a 200 G horizontal field generated from an electromagnetic coil was used to magnetize the micromagnets.[19] We then captured different concentrations of magnetic beads as surrogates for cells (8.4 μm polystyrene, Spherotech, Inc.) and found that higher bead concentrations did not affect the capture accuracy (>95%; see supplementary material[16]).

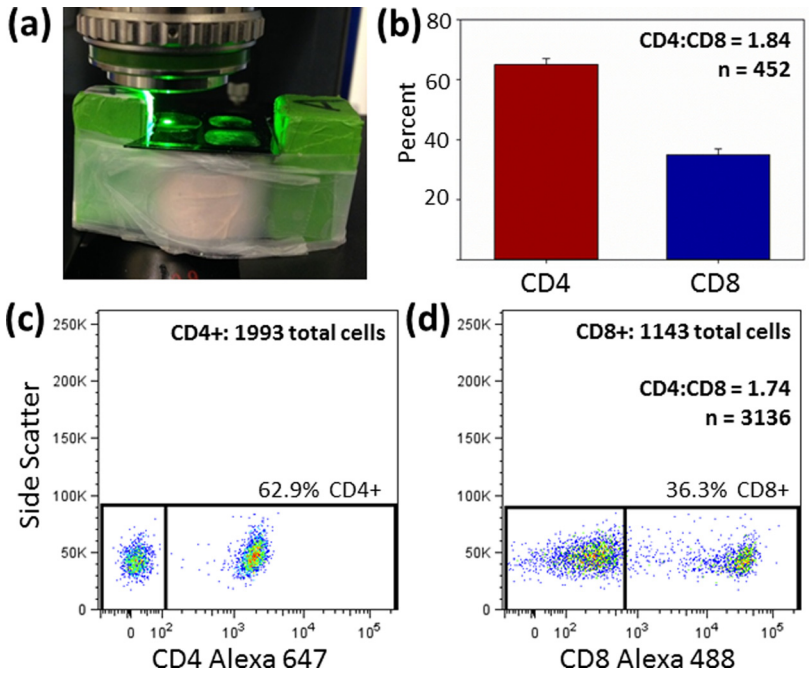

FIG. 2. CD8 analysis of CD3+ lymphocytes. (a) Photograph of the magnetographic device activated by permanent magnets (covered with green tape). The CD4:CD8 ratio determined by the (b) magnetographic microarray and (c) and (d) flow cytometry was 1.84 and 1.74, respectively.

The opposite side of each micromagnet was then populated with the second (yellow fluorescent) bead by reversing the direction of the applied magnetic field. We tested several field strengths (i.e., 10, 25, 40, or 55 G) to optimize the conditions for isolating the desired bead in the opposite well without ejecting the first bead. If the field strength was too large, the previously deposited beads could be ejected from their wells due to the repulsive magnetic force

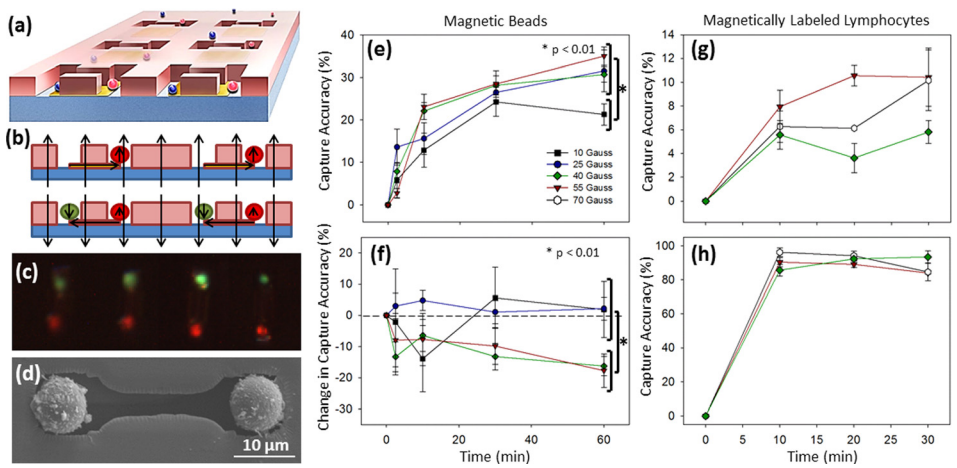

FIG. 3. Programmed pairing of magnetic beads and CD3+ lymphocytes. (a) Schematic of the magnetographic cell pair isolations. (b) Polarized micromagnets isolate cells of one type to one side in a vertical magnetic field and then cells of a second type to the other side when the field is reversed. (c) Fluorescent image of magnetically trapped green stained (top) and red stained (bottom) cell pairs. (d) SEM image of magnetically labeled cells in the microwells. (e) Capture accuracy of magnetic bead pairs. (Each color (and shape) represents the field strength of the reversed field.) (f) Change in the capture accuracy (loss) of initially captured beads after reversing the magnetic field. The capture accuracy of (g) magnetically labeled cell pairs and (h) the second magnetically labeled cell (for (e)–(h): n = 5; time starts from the deposition of the second set of cells or beads).

overcoming gravity.[12] As shown in Figure 3(e), increasing the field strength from 10 to 25 G significantly increased the capture accuracy at 60 min from the deposition of the second bead ($p < 0.01$), but increases from 25 to 55 G did not affect the capture accuracy ($p > 0.10$). As shown in Figure 3(f), higher field strengths (i.e., 40 and 55 G) resulted in lower capture accuracies compared to lower field strengths (i.e., 10 and 25 G) ($p < 0.01$), which was primarily due to ejection of the initially captured beads when the micromagnets reversed their polarity.

We then arranged pairs of membrane dyed (calcein AM, Invitrogen; PKH26, Sigma) magnetically labeled CD3+ lymphocytes. First, red stained cells (150 μl of 2×10^4 cells/ml) were deposited on the microchip in the presence of 250 G vertical magnetic field. After 20 min, the field was reversed (i.e., to 40, 55, and 70 G) and green stained cells (150 μl of 2×10^4 cells/ml) were deposited on the microchip with images taken in 10 min intervals. Fluorescence images were overlaid (Fig. 3(c)) and the capture accuracy of cell pairs was determined (ImageJ).

As seen in Figure 3(g), the capture accuracy of pairs of CD3+ lymphocytes was lower than that of magnetic beads (Fig. 3(e)). However, as shown in Figure 3(h), the second set of cells (green fluorescent) exhibited an average capture accuracy of $91.8\% \pm 1.9\%$. This indicates that the lower capture accuracy of cell pairs was either due to the ejection of initially captured (red fluorescent) cells or the migration of initially captured cells through the connecting channel, resulting from their relatively high deformability compared to magnetic beads.

In summary, we developed a simple device capable of organizing magnetic particles, cells, and pairs of cells into well-defined compartments. A major advantage of this system is the use of specific magnetic labels to both isolate cells and program their deposition. While the design of this device does not enable dynamic control of the spacing between captured cell pairs as does some dielectrophoresis-based devices,[20] it can easily capture cells with high fidelity using only permanent magnets and has clinical relevance in the assessment of immune parameters. These demonstrations potentiate a relatively simple and robust device where highly organized spatial arrangement of cells facilitates rapid and accurate analyses towards a functional and low-cost point-of-care device.

This work was supported by the NSF's Research Triangle MRSEC (DMR-1121107) and an NSF Graduate Research Fellowship (1106401) to C.W.S. We thank Marcia Bentz for her assistance for the preparation of cells, Jonathan Liu for his assistance in the fabrication of the microchips, and the staff at Duke's Shared Materials Instrumentation Facility for helpful discussions. We also thank the Duke CFAR for assistance in cell isolations and flow cytometry experiments.

[1]P. K. Chattopadhyay, T. M. Gierahn, M. Roederer, and J. C. Love, Nat. Immunol. **15**(2), 128–135 (2014).
[2]X. Cheng, D. Irimia, M. Dixon, J. C. Ziperstein, U. Demirci, L. Zamir, R. G. Tompkins, M. Toner, and W. R. Rodriguez, J. Acquir. Immune Defic. Syndr. **45**(3), 257–261 (2007).
[3]J. Nilsson, M. Evander, B. Hammarstrom, and T. Laurell, Anal. Chim. Acta **649**(2), 141–157 (2009).
[4]J. Voldman, Annu. Rev. Biomed. Eng. **8**, 425–454 (2006).
[5]C. W. Shields IV, L. M. Johnson, L. Gao, and G. P. López, Langmuir **30**(14), 3923–3927 (2014).
[6]C. W. Shields IV, D. Sun, K. A. Johnson, K. A. Duval, A. V. Rodriguez, L. Gao, P. A. Dayton, and G. P. López, "Nucleation and growth synthesis of siloxane gels to form functional, monodisperse, and acoustically programmable particles," Angew. Chem. Int. Ed. Engl. (published online) (2014).
[7]P. Tseng, J. W. Judy, and D. Di Carlo, Nat. Methods **9**(11), 1113–1119 (2012).
[8]B. B. Yellen, G. Friedman, and A. Feinerman, J. Appl. Phys. **91**(10), 8552 (2002).
[9]B. B. Yellen, G. Friedman, and A. Feinerman, J. Appl. Phys. **93**(10), 7331 (2003).
[10]B. B. Yellen and G. Friedman, J. Appl. Phys. **93**(10), 8447 (2003).
[11]B. B. Yellen and G. Friedman, Adv. Mater. **16**(2), 111–115 (2004).
[12]B. B. Yellen and G. Friedman, Langmuir **20**, 2553–2559 (2004).
[13]B. B. Yellen, O. Hovorka, and G. Friedman, Proc. Natl. Acad. Sci. U.S.A. **102**(25), 8860–8864 (2005).
[14]F. S. Fritzsch, C. Dusny, O. Frick, and A. Schmid, Annu. Rev. Chem. Biomol. Eng. **3**, 129–155 (2012).
[15]Y. Chen, P. Li, P. H. Huang, Y. Xie, J. D. Mai, L. Wang, N. T. Nguyen, and T. J. Huang, Lab Chip **14**(4), 626–645 (2014).
[16]See supplementary material at http://dx.doi.org/10.1063/1.4885840 for methods of microchip fabrication, isolation purity of CD3+ cells, and capture efficiency data of the magnetographic array.
[17]D. A. Cooper, B. Tindall, E. J. Wilson, A. A. Imrie, and R. Penny, J. Infect. Dis. **157**(5), 889–896 (1988).
[18]S. Serrano-Villar, S. Moreno, M. Fuentes-Ferrer, C. Sánchez-Marcos, M. Ávila, T. Sainz, N. G. P. de Villar, A. Fernández-Cruz, and V. Estrada, HIV Med. **15**(1), 40–49 (2014).
[19]C. W. Shields IV, S. Zhu, Y. Yang, B. Bharti, J. Liu, B. B. Yellen, O. D. Velev, and G. P. López, Soft Matter **9**(38), 9219 (2013).
[20]M. Sen, K. Ino, J. Ramon-Azcon, H. Shiku, and T. Matsue, Lab Chip **13**(18), 3650–3652 (2013).